

Spectral Angle Minimization for the Retrieval of Optically Active Seawater Constituents from MODIS Data

F. Maselli, L. Massi, M. Pieri, and C. Santini

Abstract

The application of global algorithms to optical satellite imagery often fails to correctly assess the concentrations of seawater constituents (chlorophyll, *CHL*, suspended sediments, *SS*, and yellow substance, *YS*) in spectrally complex marine environments. Additional problems may come from inaccurate radiometric, atmospheric, and geometric corrections of the remotely sensed imagery. This issue is currently analyzed using a data set of seawater samples and MODIS images taken in the Tuscany Sea (Central Italy). The analysis demonstrates that the mentioned problems mainly introduce amplitude variations in the measured reflectance. This may have negative effects on the outcome of inversion algorithms based on the minimization of conventional spectral errors. Such effects can be notably reduced by using an error index derived from the angle between measured and simulated reflectance vectors, which is insensitive to spectral amplitude variations. The potential of a classical and the new error indices is first evaluated by regressing their values against concentration differences of optically active constituents found over the available sample pairs. The performance of the two error indices are then assessed within an inversion algorithm applied to the same samples. The results obtained show the potential of the new error index particularly to improve the estimation of *CHL* concentration.

Introduction

The assessment of sea biophysical properties is important not only for an effective and sustainable management of marine ecological resources, but also to assure the quality of bathing waters and prevent environmental hazards and pollution. The relevance of such an assessment has recently increased in order to characterize the complex interactions between climate change and the global carbon cycle (IPCC, 2001).

Satellite remote sensing techniques provide an efficient tool to estimate the concentrations of ecologically important seawater constituents with potentially high spatial and temporal resolutions. Remote sensing of sea optical features is based on the study of the reflective properties of the main optically active seawater constituents: *phytoplankton* (*PH*),

whose concentration is generally estimated by *chlorophyll-a* (*CHL*); non algal particle (*NAP*), which in coastal waters is mostly represented by *suspended sediments* (*SS*); and *yellow substance* (*YS*), also named colored dissolved organic matter (*CDOM*) (IOCCG, 2000). In shallow waters, bathymetry and benthic optical properties also play a major role, and the bottom reflectance must be considered (Lee and Carder, 2002; Maselli *et al.*, 2005).

Radiative transfer theory provides the link between the inherent optical properties (IOPs), like the absorption and scattering coefficients of seawater constituents, and the apparent optical properties (AOPs), like the remote sensing reflectance (R_{rs}) measured by sensors above the sea surface (Chang *et al.*, 2003). The same theory provides the solution of the direct problem, i.e., computing AOPs from IOPs. Conversely, the estimation of IOPs, given AOPs, the so-called inverse problem, is more complicated due to conceptual and practical problems related to the uniqueness and stability of the possible solutions (Mobley, 1994). In fact, the knowledge of the radiance above the sea surface in one direction does not allow the accurate assessment of the parameters which determine the IOP's (IOCCG, 2006).

In spite of these difficulties, various semi-analytical ocean color inversion algorithms have been proposed and applied successfully (Maritorena *et al.*, 2002; Carder *et al.*, 2004). Most of these algorithms are based on the finding of Gordon *et al.* (1975) and Morel and Prieur (1977) that the remote sensing reflectance is proportional to the backscattering coefficient (b_b) and inversely proportional to the sum of the absorption (a) and the backscattering coefficients. This finding allows the development of relatively simple inversion algorithms that identify simulated reflectance which best correspond to the measured spectral data.

The performance of estimation methods based on these algorithms are generally good in deep ocean, or Case 1, waters (phytoplankton dominated), but are poorer in optically complex, or Case 2, waters (sediment and/or yellow-substance dominated) (Darecki and Stramski, 2004). Particular difficulties may come from the presence of seawater constituents showing spatially or temporally variable spectral features, which complicate the interpretation of the acquired signal (Babin *et al.*, 2003a). Additional problems are found in turbid coastal areas, where standard

F. Maselli and C. Santini are with IBIMET-CNR, Via Madonna del Piano 10, 50019 Sesto Fiorentino (FI), Italy (maselli@ibimet.cnr.it).

L. Massi is with the Laboratorio di Ecologia, Dipartimento di Biologia Vegetale, Università di Firenze, Italy.

M. Pieri is with Consorzio LaMMa, Firenze, Italy.

Photogrammetric Engineering & Remote Sensing
Vol. 75, No. 5, May 2009, pp. 595–605.

0099-1112/09/7505-0595/\$3.00/0
© 2009 American Society for Photogrammetry
and Remote Sensing

atmospheric correction algorithms generally fail to produce reliable results due to the violation of the basic assumption that water leaving radiances are close to zero in near-infrared wavebands (Ruddick *et al.*, 2006; Shanmugan and Ahn, 2007).

The Mediterranean Sea is a typical example where global inversion algorithms need to be improved (Ouillon and Petrenko, 2005; Zibordi *et al.*, 2006; Volpe *et al.*, 2007). This necessity was confirmed for the Tuscany Sea by a recent investigation of our research group, which demonstrated that daily standard MODIS products poorly estimate the concentrations of chlorophyll, suspended sediments and yellow substance (Santini *et al.*, 2004). In particular, these products strongly overestimate the concentrations of CHL and YS, while underestimate that of SS.

The current work analyses this issue using a data set of seawater samples and MODIS data taken near the coast of the Tuscany Sea in 2003. Next, a modification of conventional inversion algorithms is proposed in order to reduce the effects of the problems found. The performance of the conventional and modified retrieval methodologies are finally evaluated by applying various statistical analyses to the available seawater and reflectance samples.

The paper is organized as follows. The next section introduces the theoretical background of ocean optics which is needed to compute measured and simulated seawater reflectance. The main features of the study area and data are then described. Next, the data processing and results achieved are exposed in such a way to respect the logical sequence of the experiments performed. Conclusions are finally drawn about the possible advantages and limitations of the methodologies analyzed.

Theoretical Background

Omitting hereafter the dependency on the wavelength, the water leaving radiance (L_w), which is the basic radiometric quantity in remote sensing of sea color, can be defined as the radiance emerging from the sea, just above the water-air interface, in the direction of the sensor. The radiance measured by satellite is transformed, after atmospheric correction, into the normalized water leaving radiance (nL_w).

The remote sensing reflectance (Rrs), another basic term for many ocean-color algorithms, is the ratio of water leaving radiance to downwelling irradiance just above the sea surface. Rrs_{meas} can be considered as the reflectance which is directly measured by remote sensors like MODIS, and can be computed by dividing the normalized water leaving radiance, a standard MODIS data product, by the solar irradiance (F_0) at top of the atmosphere (Morel and Bélanger, 2006):

$$Rrs_{meas} = \frac{nL_w}{F_0} \quad (1)$$

where the values of F_0 relative to Terra and Aqua MODIS are reported in the Ocean color Website, URL: <http://oceancolor.gsfc.nasa.gov>.

As mentioned previously, the remote sensing reflectance can be simulated relying on consolidated theory and experimental findings. In particular, the simulated remote sensing reflectance (Rrs_{sim}) can be approximately represented as a function of inherent optical properties (Morel and Gentili, 1996):

$$Rrs_{sim} = \mathfrak{R} \frac{f}{Q} \frac{b_b}{a} \quad (2)$$

where \mathfrak{R} is a dimensionless quantity that includes transmission and reflection phenomena at the water-air interface, f is

a function of the water optical properties and of illumination conditions, Q is the ratio of upwelling irradiance divided by the zenith propagating upwelling radiance both evaluated just beneath the sea surface, and b_b and a are the total backscattering and absorption coefficients, respectively. Because f and Q follow similar trends with changing sun angle, the range of variation in their ratio is considerably reduced (Morel and Gentili, 1996). In our case, an \mathfrak{R} equal to 0.54 and f/Q equal to 0.0949 were used in accordance to Carder *et al.* (2003).

The total absorption a and total backscattering b_b coefficients can be split into the contributions of the optically active components of the seawater, and expressed as a linear function of their concentrations. Given that the main components in the absorption process are: phytoplankton, suspended sediments, yellow substance, and water itself, the total absorption can be expressed as:

$$a = a_w + [\text{CHL}] \cdot a_{PH}^* + [\text{SS}] \cdot a_{NAP}^* + [\text{YS}] \cdot a_{YS}^* \quad (3)$$

where a_w is absorption coefficient of pure seawater, a_{PH}^* , a_{NAP}^* , and a_{YS}^* represent the specific absorption coefficients of phytoplankton, suspended sediments and yellow substance, respectively, and [CHL], [SS] and [YS] are the concentrations of phytoplankton and suspended sediments and the value of the absorption coefficient of yellow substance, respectively. Likewise, considering null the contribution of YS to diffusion, the total backscattering coefficient can be expressed as:

$$b_b = b_{bw} + [\text{CHL}] \cdot b_{PH}^* + [\text{SS}] \cdot b_{NAP}^* \quad (4)$$

where b_{bw} is backscattering coefficient of pure seawater, and b_{PH}^* , b_{NAP}^* are the specific backscattering coefficients of phytoplankton and non algal particle.

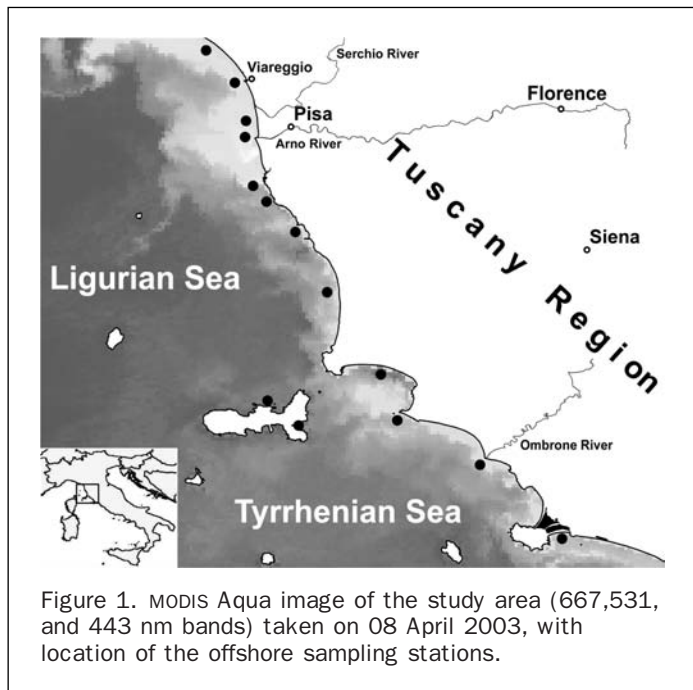
The simulated remote sensing reflectance (Rrs_{sim}) can thus be obtained as:

$$Rrs_{sim} = 0.051 \cdot \frac{b_{bw} + [\text{CHL}] \cdot b_{PH}^* + [\text{SS}] \cdot b_{NAP}^*}{a_w + [\text{CHL}] \cdot a_{PH}^* + [\text{SS}] \cdot a_{NAP}^* + [\text{YS}] \cdot a_{YS}^*} \quad (5)$$

These formulas were the basis for the current comparative analysis of measured and simulated remote sensing reflectance. The former, Rrs_{meas} , was derived from MODIS images by using Equation 1, while the latter, Rrs_{sim} , was computed through Equation 5. In the simulations, b_{bw} was taken from Smith and Baker (1981) and a_w from Pope and Fry (1997), while the specific absorption and backscattering coefficients were derived from the analysis of the available sea reference data as described in the next sections.

Study Area

The study area corresponds to the sea in front of the Tuscany Region, Central Italy (Figure 1). This sea area is located in a transition zone between two basins, the Ligurian in the North and the Tyrrhenian in the South. Some differences emerge between the two basins, particularly because of climate and bathymetry. Water exchanges between the two basins generally occur toward the Ligurian Sea especially in winter and spring. The littorals are mostly low and sandy with weak bottom slope and shallow depth. Exceptions are represented by some high and rocky coasts in the center and South of the region. The Arno and Serchio Rivers in the North and the Ombrone River in the South mostly determine the features of the coastal waters around the respective mouths (Figure 1).



Several studies carried out in different sea areas in front of Tuscany show that the annual cycle of phytoplankton biomass can be characterized by two maxima in spring and in fall (Innamorati *et al.*, 1993), or by a unique bloom from fall to late spring (Innamorati *et al.*, 2003). The Tuscany Sea generally shows oligotrophic features that are less evident in the North. In the southern sea, phytoplankton biomass maxima can be of 0.5 to 1 mg/m³ of *chlorophyll-a* at the end of winter / beginning of spring. In the northern sea these values are higher, up to 2.5 mg/m³. Minimum concentrations are typically found in summer and range from 0.07 to 0.15 mg/m³. Near the largest river mouths, CHL can be higher than 5 mg/m³. In these more eutrophic areas minimum CHL rarely drops to 1 mg/m³, and the regularity of the phytoplankton temporal cycle can fail. This can result in a growth impulse series, irregularly distributed during the year, and generally correlated with the river flow. Innamorati *et al.* (1993), relating several optical features of the sea around the Tuscan Archipelago, show that these waters generally belong to Case 1. Case 2 waters instead prevail in coastal areas especially near sandy littorals and river mouths where the suspended detrital particles and dissolved organic matter are determinant for light attenuation.

Collection and Analysis of Sea Data

Collection of Sea Data

The water samplings were carried out by the Regional Agency for Environmental Protection of Tuscany (ARPAT) in seven cruises from April to October 2003. The sampling stations were located in pairs along 14 transects perpendicular to the coastline (Figure 1). The coastal stations were placed at about 500 m from the shoreline, and the others at about an additional 3,000 m. The bottom depth varies from several meters to 20 m for the coastal stations and from 15 to 50 m for the offshore stations. To avoid the effect of the sea bottom and of the land on the spectral signatures of the examined samples, only those taken in the offshore stations were currently considered. All sea water samples were collected at about 0.5 m from the sea surface by means of Niskin bottles.

Determination of CHL, YS, and SS Concentrations

All applied preservation procedures and analysis protocols are compliant with those recommended for SeaWiFS activities (Mueller and Austin, 1995). In particular:

- Concentration of *chlorophyll-a* (CHL) in seawater was determined after filtration on Whatman GF/F filters (Ø 25 mm), by spectrofluorimetric analysis (PERKIN-ELMER LS5B) according to Holm-Hansen *et al.* (1965).
- Yellow substance (YS), or CDOM optical density, was measured by a SHIMADZU UV250PC spectrophotometer with quartz cells of 10 cm of pathlength after filtration on 0.2 µm Nuclepore PC membrane (Bricaud *et al.*, 1981; Babin *et al.*, 2003b). The absorption spectra of YS were calculated (Bricaud *et al.*, 1981) from optical density corrected for scattering according Davies-Colley and Vant (1987). The whole spectra were reconstructed following Babin *et al.*, (2003b). The absorption coefficient (m⁻¹), at 400 nm, was utilized as an estimate of YS. The yellow substance specific absorption spectrum ($a_{YS}^*(\lambda)$) was obtained dividing $a_{YS}(\lambda)$ by $a_{YS}(400)$.
- The gravimetric analysis of suspended sediments (SS) was performed following Strickland and Parson (1972) modified by Van der Linde (1998) for the salt washing procedure of the filter (Whatman GF/F filters, Ø 47 mm).

The results of these analyses confirmed that CHL was highest at the station near the Arno mouth (up to 3 mg/m³). High concentrations (1.1 to 0.6 mg/m³) were also found in the northern area, in front of the city of Viareggio. In the other stations, CHL ranged between 0.1 and 0.5 mg/m³. Superimposed on the local maxima near the river mouths a general decreasing trend of CHL from North to South was evident. SS ranged from 4 to 15 mg/l, and the distribution of SS showed increasing values near the main river mouths and a general decreasing trend from North to South. On average 80 percent in weight of suspended sediments was given by inorganic substances. YS absorption at 400 nm ranged from 0.012 to 0.51, with the average around 0.12 m⁻¹. YS showed a distribution similar to those of CHL and SS, with sharp increases near the coastline and the main river mouths.

Estimation of Absorption Coefficients

The absorption coefficient spectra of total particulate matter, a_P , were determined utilizing the transmittance-reflectance (T-R) method (Tassan and Ferrari, 1995). Whatman GF/F filters were used, together with a LI-COR LI 1800UW spectroradiometer equipped with an integrating sphere (LI 1800-12S). A correction for path-length amplification factor (β) was performed following Bricaud and Stramski (1990). Non-algal particle absorption coefficient, a_{NAP} , was measured on the same filters after absolute methanol extraction of pigments (Kishino *et al.*, 1985). In all cases, absorption coefficient spectra with 1 nm spectral resolution were obtained. Phytoplankton absorption coefficient, a_{PH} , were computed by subtraction: $a_{PH} = a_P - a_{NAP}$. Phytoplankton *chlorophyll-a*-specific (cross section) absorption coefficients, a_{PH}^* , were calculated by dividing each a_{PH} spectrum by the CHL in the sample. Likewise, specific absorption of non algal particle a_{NAP}^* was calculated dividing a_{NAP} by the SS.

The bulk and spectral variability of specific absorption spectra of phytoplankton, non-algal particle and YS in the sampling area were characterized by computing the ensemble mean, standard deviation and coefficient of variation of the available samples. The results obtained are shown in Figure 2a through 2c. Phytoplankton-specific absorption spectra (Figure 2a) showed a mean coefficient of variation (C.V.) of 32 percent. The lowest C.V. values were in the *chlorophyll-a* absorption band, while in the green band the C.V. increased reaching a maximum (48 percent) at 570 nm. The ensemble variability of non-algal particle-specific

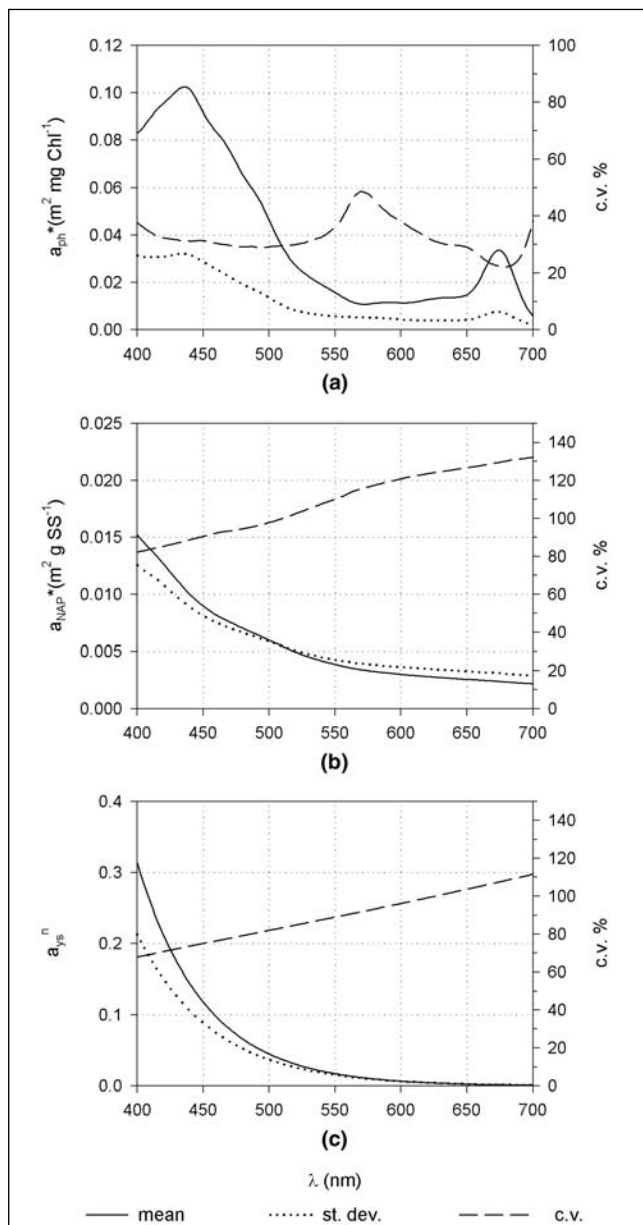


Figure 2. Specific absorption coefficients of (a) phytoplankton and (b) non-algal particle and (c) normalized (by spectral average) absorption coefficient of γ_s . The means, standard deviations, and coefficients of variation of the spectra found over all offshore samples are reported.

absorption spectra (Figure 2b) was very high (C.V. spectral average of approximately 105 percent), particularly in the red part of the spectrum. The absorption spectra of yellow substance, normalized by their spectral average (300 to 700 nm) (Figure 2c), also showed high C.V. (90 percent, higher in the red part of the spectrum).

These results indicate that all three seawater constituents, and particularly non-algal particle and yellow substance, were characterized by a very high variability of their specific absorption coefficients. The spectral dimensionality of this variability was investigated by applying Principal Component Analysis (PCA) to the specific absorption spectra of non-algal particle, yellow substance, and phytoplankton. Since the

TABLE 1. AVERAGE ABSORPTION COEFFICIENTS COMPUTED FROM ALL OFFSHORE SAMPLES

Wavelength (nm)	a_{PH}^*	a_{NAP}^*	$a_{\gamma_s}^*$
412	0.075663	0.014400	0.771887
443	0.082464	0.010080	0.396018
488	0.050027	0.006791	0.150871
531	0.019442	0.004583	0.060239
551	0.013675	0.003924	0.039354
667	0.028009	0.002537	0.003384
678	0.030643	0.002445	0.002686

original resolution of the spectra (1 nm) was retained, PCA was applied to 301 - 1 nm spectral bands (from 400 to 700 nm).

The first principal component accounted for 98 percent and 95 percent of the total variance of non-algal particle and yellows substance, respectively, with the other components being of marginal importance. In the case of phytoplankton, the first, second, and third components accounted for 73 percent, 15 percent and 7 percent of the total variance, respectively. This indicates that the found absorption variability of non-algal particle and yellows substance was fundamentally one-dimensional, i.e., almost completely related to amplitude variations of absorption efficiency, while changes in shape were of negligible importance. The situation was different for phytoplankton, where significant fractions of the total variance were explained by the second and the third components. This indicates that changes in shape of the phytoplankton absorption spectra were not negligible.

Mean specific absorption coefficients were computed for the seven MODIS visible bands by averaging the values of all samples. These coefficients, which were used for the following simulation exercises, are reported in Table 1.

Estimation of Backscattering Coefficients

Measurements of scattering or backscattering coefficients were not made due to the difficulty in analytically determining these quantities. As the backscattering terms were necessary to calculate Rrs_{sim} , the contribution of non-algal particle and phytoplankton to total backscattering was indirectly estimated.

Irradiance reflectance measurements by a LI-COR LI 1800UW spectroradiometer were sporadically taken at the sea surface and at several depths underwater. From these measurements, reflectance (R) and vertical attenuation coefficient of irradiance (Kd) were obtained. According to Kirk (1989 and 1994), the diffuse backscattering coefficient (b_{bd}) was estimated multiplying these quantities by a constant ($b_{bd} \approx 3.5 R Kd$). Estimates of the backscattering coefficient were obtained dividing the diffuse backscattering coefficient by a variable factor which was computed as a function of measured reflectance following again Kirk, (1989, Figure 8). Such estimates are close to those obtained by Loisel and Stramski (2000). The non-algal particle specific backscattering coefficients, b_{NAP}^* , were computed dividing b_b by suspended sediment concentration. The obtained values of b_{NAP}^* centered on the MODIS bands are reported in Table 2. These estimates are coherent with that already published for coastal waters (Babin *et al.*, 2003b; Zawada *et al.*, 2007).

The same table summarizes the specific backscattering coefficients of phytoplankton centered on the MODIS bands, b_{PH}^* , which were taken from Vaillancourt *et al.* (2004).

Collection and Preprocessing of Satellite Data

Level-2 MODIS products, which are freely distributed by NASA, were utilized as satellite data. These are Local Area Coverage (LAC) images with a pixel resolution of 1 km, which

TABLE 2. AVERAGE BACKSCATTERING COEFFICIENTS COMPUTED BY THE METHODOLOGY DESCRIBED IN THE TEXT

Wavelength (nm)	$b_{b_{PH}}^*$	$b_{b_{NAP}}^*$
412	0.00130	0.00295
443	0.00120	0.00305
488	0.00098	0.00295
531	0.00089	0.00269
551	0.00083	0.00246
667	0.00078	0.00137
678	0.00080	0.00180

are already corrected for the atmospheric effect. Five Terra-MODIS scenes and six Aqua-MODIS scenes were selected coincident with the dates of the sea samplings (Table 3). The Terra MODIS ocean products contained the normalized water leaving radiances in seven optical bands. The images were georeferenced using ground control points. The Aqua MODIS standard products contained the six bands of normalized water leaving radiances (the 678 nm band is not provided as standard Level-2 product). These images were georeferenced using the attached ancillary information. The geometric accuracy of all images was assessed through superimposition of a Tuscany coastline vector file. The mean accuracy was found to be around one pixel (1 km), which was deemed sufficient to approximately localize the sampling points more distant from the coastline. These sampling points (21 for Terra and 22 for Aqua) were superimposed on the georeferenced images, and the water leaving radiances were extracted from the corresponding pixels. The application of Equation 1 allowed the computation of remote sensing reflectances in seven channels for Terra data, and in six channels for Aqua data. The main statistics of these data are summarized in Table 4. In general, the remote sensing reflectances found were quite regular and within reasonable ranges. Negative values were however found for some samples at higher wavelengths.

Comparative Analysis of Sea and Satellite Data

Computation and Comparison of Measured and Simulated Reflectances

The concentrations of the three optically active seawater constituents in the study samples were combined through Equation 5 with the average optical properties of Tables 1 and 2 to compute the simulated remote sensing reflectances of all samples in the Terra and Aqua bands. These simulated reflectances were compared to relevant measured (MODIS) reflectances by computing per-band correlation coefficients (r) and root mean square errors (RMSE). The results of such comparisons are summarized in Table 5. The accordance between the two reflectance series was generally rather poor, particularly for the bands at lower wavelengths (412 to 443 to 488 nm). Similar results were obtained using Aqua and Terra data.

TABLE 3. SELECTED TERRA AND AQUA SATELLITE SCENES

Water sampling date	Terra overpass	Aqua overpass
08/04/2003	*	*
29/05/2003		*
01/07/2003	*	*
15/09/2003	*	*
16/09/2003		*
17/09/2003	*	
10/10/2003	*	*

TABLE 4. REFLECTANCE STATISTICS OF THE 21 TERRA AND 22 AQUA SAMPLES

Terra				
Wavelength (nm)	Average	Standard deviation	Minimum	Maximum
412	0.00601	0.00308	0.00055	0.01594
443	0.00834	0.00342	0.00300	0.01781
488	0.01133	0.00472	0.00458	0.02157
531	0.00976	0.00587	0.00234	0.02279
551	0.00869	0.00592	0.00147	0.02216
667	0.00081	0.00109	-0.00234	0.00383
678	0.00084	0.00106	-0.00212	0.00360
Aqua				
Wavelength (nm)	Average	Standard deviation	Minimum	Maximum
412	0.00610	0.00242	0.00280	0.01355
443	0.00864	0.00354	0.00375	0.01958
488	0.01065	0.00494	0.00359	0.02486
531	0.00938	0.00648	0.00123	0.02799
551	0.00838	0.00638	0.00079	0.02664
667	0.00094	0.00176	-0.00193	0.00745

TABLE 5. CORRELATION COEFFICIENTS AND RMSES FOUND BY COMPARING MODIS AND SIMULATED REMOTE SENSING REFLECTANCES OF 21 TERRA AND 22 AQUA SAMPLES

Terra		
Wavelength (nm)	r^2	RMSE
412	0.072	0.0038
443	-0.061	0.0046
488	-0.074	0.0057
531	0.565**	0.0055
551	0.629**	0.0051
667	0.547*	0.0010
678	0.557**	0.0011
Aqua		
Wavelength (nm)	r^2	RMSE
412	0.059	0.0031
443	0.000	0.0042
488	0.109	0.0058
531	0.564**	0.0060
551	0.611**	0.0055
667	0.444*	0.0016

* = Significant Correlation, $P < 0.05$;

** = Highly Significant Correlation, $P < 0.01$

In addition to the possible errors which may come from the approximations used in our simulation strategy, the poor accordance between measured and simulated reflectances can be attributed to several possible causes:

- Inaccurate radiometric and atmospheric corrections of the MODIS images. The latter in particular is a well know error source for data derived from optical satellite imagery. All correction procedures used are in fact based on approximate modeling of the atmospheric contribution to downwelling irradiance and upwelling radiance (Siegel *et al.*, 2000; Bailey and Werdell, 2006). A clear indication of such problems in the current case was the finding of negative MODIS

reflectances for some points, which were most likely due to radiometric noise or overcorrection of atmospheric scattering.

- Geometric inaccuracy in positioning the sampling points on the images, which leads to a bad correspondence between seawater and MODIS samples. This is caused by the different spatial representation of the two samples, since seawater constituents are measured in specific points, while MODIS pixels refer to an area of 1 km². The likely relevance of the first factor in the current case was indicated by the mean geometric error of one pixel found in the preliminary image quality assessment, whose effect was presumably exacerbated by the high spatial variability in bio-chemical features which is typical of most coastal waters.
- Spatial or temporal optical variability of sea water constituents (i.e., variation in absorption and scattering properties of PH, NAP, and YS). This is also a major error source in areas which are strongly affected by the presence of water constituents of different origins (river and channel outflows, urban and industrial discharges, etc.). The current importance of this factor was indicated by the high specific absorption variability previously found, particularly for NAP and YS. As previously seen, this variability was mostly due to changes in amplitude of the absorption spectra, which presumably lead to similar changes in reflectance features of the examined samples.
- Other possible environmental error sources, such as those due to sun glint (reflection from the water surface), to the presence of waves, bubbles, and whitecaps or to the influence of the sea bottom (IOCCG, 2006). The importance of these factors is generally difficult to quantify, but can be expected to occasionally become not marginal in coastal environments which are only relatively far from the shoreline (about 3 km) and where the depth of the sea bottom may be lower than 25 m.

The effect of these possible error sources on the measured remote sensing reflectances was analyzed by computing the ratios of measured over simulated reflectances (Rrs_{meas} / Rrs_{sim}) for all sample points and wavebands. As expected, these ratios showed great variations, ranging from almost 0 to about 5. It was observed, however, that these spectral ratios varied mostly in a parallel way, i.e., that MODIS reflectances were usually uniformly lower or higher in all bands with respect to simulated reflectances. This observation was quantitatively tested by applying again Principal Component Analysis to the 21 ratios of Terra data and the 22 ratios of Aqua data. The results of the analyses indicated that the first principal components of the spectral ratios accounted for very high percentages of the total variances (about 86 percent for the seven-band Terra data and 93 percent for the six-band Aqua data). Moreover, the eigenvectors of these components approximated normal averages of the original bands.

These findings are a clear indication that MODIS spectral signatures differed from simulated remote sensing reflectances fundamentally due to amplitude variations. Most of these variations were attributable to the previously found absorption amplitude variability of the main seawater constituents. The effect of such variability was presumably reinforced by possible inaccuracy in the radiometric and atmospheric corrections applied to the images, which may affect all bands in a similar way.

Consideration of Different Error Indices

The previous observations have important consequences on the potential of conventional IOP's retrieval algorithms based on the minimization of the differences between measured and simulated spectral reflectances. These algorithms are generally based on the simulation of a large number of spectral reflectances obtained through the previously exposed theory by varying the concentrations of the main constituents. The similarity of measured and simulated

reflectances is then computed by means of a classical error index, such as the RMSE:

$$RMSE_{M,S} = \sqrt{\frac{\sum_{i=1}^{NB} (Rrs_{meas} - Rrs_{sim})^2}{NB}} \quad (6)$$

where $RMSE_{M,S}$ is the root mean square error between measured and simulated reflectances found over NB bands. This process allows the identification of an error minimum, which corresponds to the sea water constituent concentration estimates which are finally outputted. As can be easily understood, $RMSE_{M,S}$ can be strongly affected by the amplitude variations of measured reflectances which were found in the present case. Consequently, inversion algorithms based on its minimization are expected to fail in correctly identifying the error minima corresponding to measured water constituent concentrations.

Such a problem could be overcome by the use of an error minimization criterion which is intrinsically insensitive to reflectance amplitude variations. The theory which can provide such a criterion is that of Spectral Angle Analysis (Sohn and Rebello, 2002; Chang *et al.*, 2006). This technique considers two series of multivariate observations as vectors in a corresponding multidimensional space, and defines the similarity between these vectors by measuring the spectral angle between them. More specifically, the cosine of the angle between the vectors of measured and simulated reflectances, $\cos\theta_{M,S}$ can be found as:

$$\cos\theta_{M,S} = \frac{Rrs_{meas}^T Rrs_{sim}}{\|Rrs_{meas}\| \|Rrs_{sim}\|} \quad (7)$$

where Rrs_{meas} and Rrs_{sim} are the vectors of measured and simulated reflectances in NB bands, respectively. From a statistical viewpoint, $\cos\theta_{M,S}$ is equivalent to the correlation coefficient between the two reflectance series. Similarly to this, it can vary from -1 (complete negative agreement) to $+1$ (complete positive agreement). A main property of this transform is its complete insensitivity to reflectance amplitude variations. In other terms, $\cos\theta_{M,S}$ measures the similarity in shape between the two reflectance vectors without detecting amplitude spectral differences. The application of this error index was therefore expected to reduce the influence of the above mentioned problems.

Preliminary Evaluation of Spectral Error Indices

The consequences of applying the two error indices to the current experimental data were preliminarily evaluated by using them to rank all possible pairs of sample points in comparison to corresponding concentration differences of the three water constituents. To this aim, the absolute differences in concentration of the three seawater constituents were computed for all pairs of measured reflectances (i.e., for 21²/2-21 points for Terra data and for 22²/2-22 points for Aqua data). Next, the corresponding $RMSE_{M,S}$ and $\cos\theta_{M,S}$ were computed for the same sample pairs using the relevant MODIS reflectances. The agreement between the concentration differences and the two error indices was assessed by linear correlation analysis.

The results of the analysis are summarized in Figure 3 as determination coefficients (r^2) between concentration differences and error indices. These results show that the use of the conventional error index produced very poor agreements between spectral and bio-physical differences. This is particularly the case for CHL and YS, while some

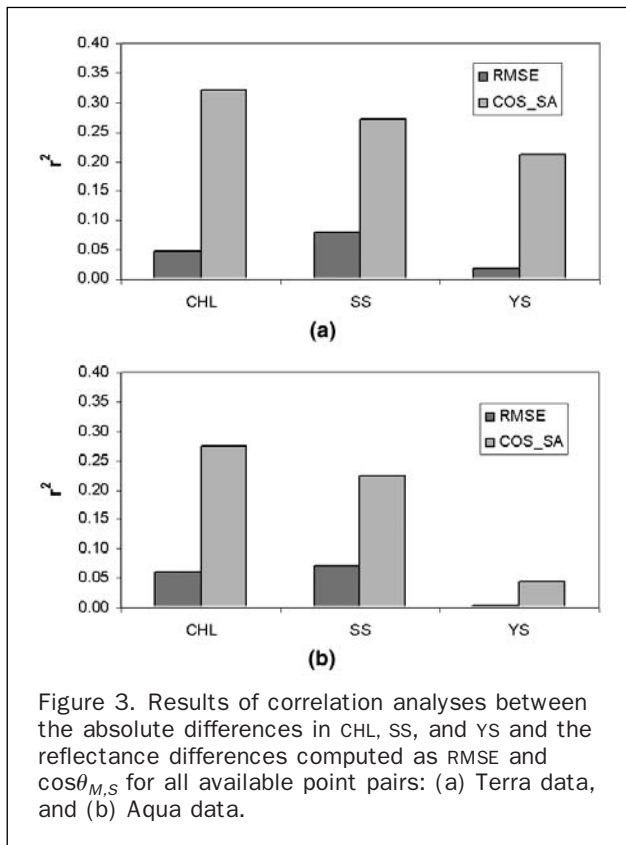


Figure 3. Results of correlation analyses between the absolute differences in CHL, SS, and YS and the reflectance differences computed as RMSE and $\cos\theta_{M,S}$ for all available point pairs: (a) Terra data, and (b) Aqua data.

marginal correlation existed for SS. The determination coefficients were highly improved for all three constituents using $\cos\theta_{M,S}$, both for Terra and Aqua data. This was a first indication that the new error index was markedly more informative than $RMSE_{M,S}$ on the concentrations of some water constituent of the examined samples.

Estimation of Water Constituent Concentrations

The results of the previous trial supported the application of the new error index to retrieve the concentrations of the three main seawater constituents for all available samples. A specific FORTRAN program was therefore written which simulated a large number of possible reflectances for each estimation point (MODIS pixel) by varying [CHL], [YS], [SS] within Equation 6. More precisely, 100 concentrations of each constituents were considered within ranges given by the sea measurements (0.05 to 5.0 mg/m³ for [CHL], 0.5 to 50.0 mg/l for [SS], and 0.005 to 0.5 m⁻¹ for [YS]), for a total of $100^3 = 1,000,000$ simulated reflectances for each estimation point. The specific absorption and scattering coefficients necessary for Equation 5 were again those reported in Tables 1 and 2. The simulated reflectances were then compared to the sample reflectances by using the two error indices. The concentrations of CHL, YS, and SS corresponding to the minimum $RMSE_{M,S}$ or maximum $\cos\theta_{M,S}$ were finally kept and evaluated against the measured concentrations by means of correlation coefficient and RMSE statistics. The results of this experiment are shown in Figure 4a through 4f and Figure 5a through 5f for the Terra and Aqua data, respectively. The algorithm based on the minimization of $RMSE_{M,S}$ was only capable of approximately estimating [SS], while it gave inferior results for both [CHL] and [YS]. More specifically, the estimation of [SS] was relatively accurate in terms of both statistics used. On the contrary,

the correlations between measured and estimated [CHL] were very low, and this concentration was strongly underestimated. Higher correlations were found for [YS], which was however markedly overestimated. These patterns can be attributed to the predominance of the spectral signatures of NAP in the considered waters, which could obscure the signatures of the other constituents. NAP are in fact known to exert a major influence on the reflectance of marine coastal waters (Ahn *et al.*, 2001), and, in the specific case, they were the seawater constituent whose concentration was most correlated with spectral variations measured as $RMSE_{M,S}$ (Figure 3).

In general, the estimation accuracies were improved when using the algorithm based on the maximization of $\cos\theta_{M,S}$. Specifically, the estimation of [CHL] was notably enhanced in terms of both r and RMSE, up to reaching a high accuracy level. The improvement was more variable for [SS], since r was increased in both cases, but a significant decrease in RMSE was obtained only with Terra data. In the case of [YS] there was no accordance between the changes in the two accuracy statistics considered (r^2 and RMSE) when using Terra and Aqua data. In one case (Terra) [YS] remained notably overestimated, while in the other the estimation capability of the new algorithm was rather uncertain.

The new algorithm was finally applied to all seawater pixels of the available MODIS imagery to produce images describing the concentrations of the three seawater constituents. Possible spatial irregularities in the output images were reduced by the application of a Gaussian filter. Examples of filtered concentration images, referred to the same MODIS scene of Figure 1, are shown in Figure 6a through 6c. These images depict a typical situation of Tuscany Sea in spring, when CHL and SS reach high levels only in the adjacency of the mouths of the main rivers (particularly Arno and Serchio in the North of the region), while YS is more uniformly high near the coastline.

Discussion and Conclusions

Estimating the concentrations of optically active seawater constituents is important for both scientific and practical reasons. While the sensors mounted onboard the first Earth resource satellites were unsuited to precisely define the optical characteristics of seawaters, most recent satellite sensors have brought significant improvement in this field. The MODIS system, in particular, was envisaged to produce, among the others, regular estimates of optically active sea water constituents over the entire globe. This operation is now routinely performed through the application of a processing chain based on consolidated ocean optics theory.

The algorithms used for this task, however, were developed to work on a global scale and do not comply with the optical variability of seawater constituents which is typical of specific marine areas. Further problems may come from other common error sources, such as the inaccurate atmospheric correction of the remote sensing data, which is particularly frequent in marine coastal areas. The current work showed that these problems may lead to amplitude reflectance variations in the optical characteristics of Tuscany coastal seawaters. This finding supports the utilization of empirical algorithms based on the use of spectral band ratios, which remove the effects of spectral amplitude variations (O'Reilly *et al.*, 1998 and 2000). Such algorithms, however, do not fully exploit the potential of spectral observations, since they use only the information contained in two to three bands. Moreover, these algorithms are generally unsuited to contemporaneously estimate the

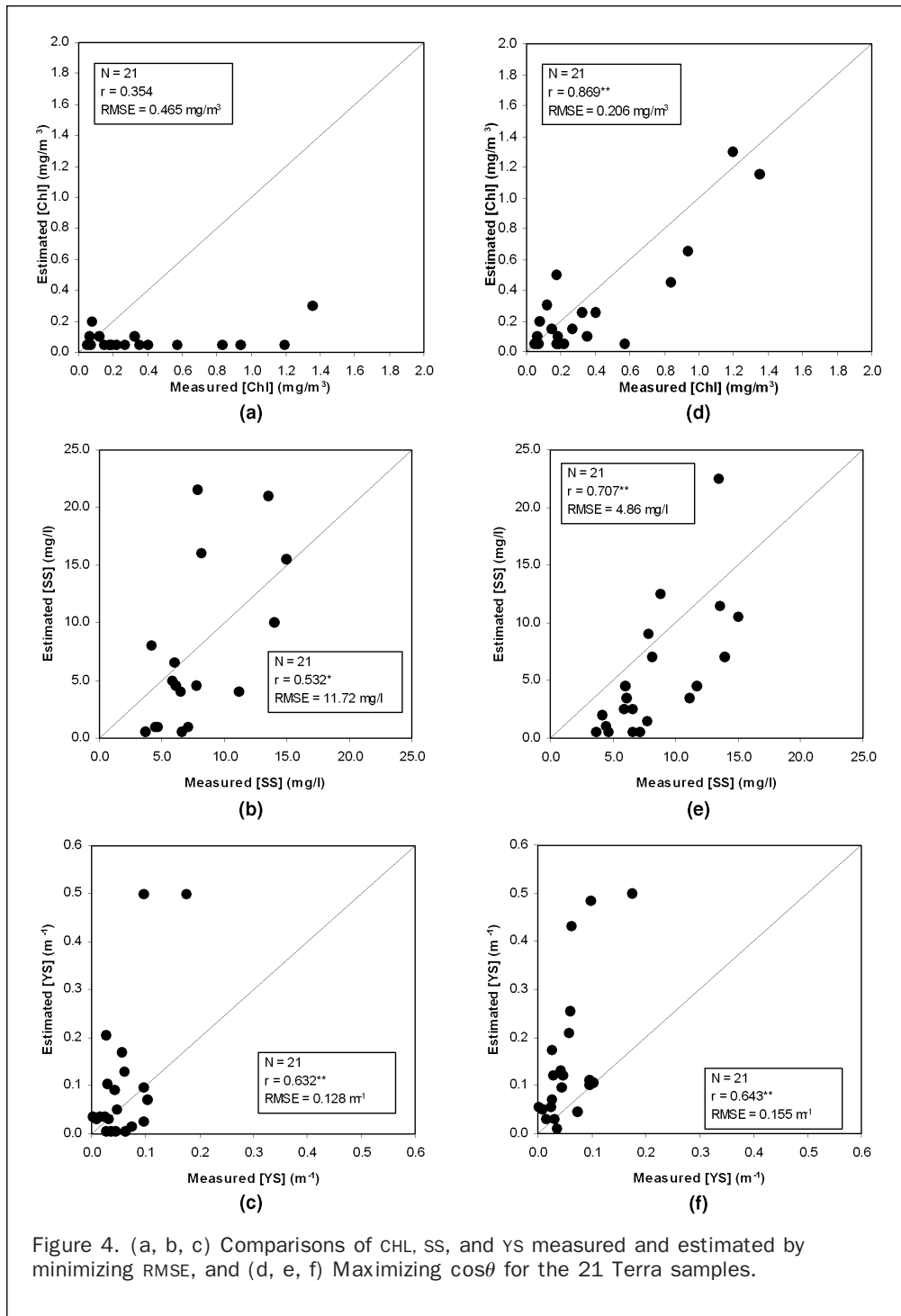


Figure 4. (a, b, c) Comparisons of chl, ss, and ys measured and estimated by minimizing RMSE, and (d, e, f) Maximizing $\cos\theta$ for the 21 Terra samples.

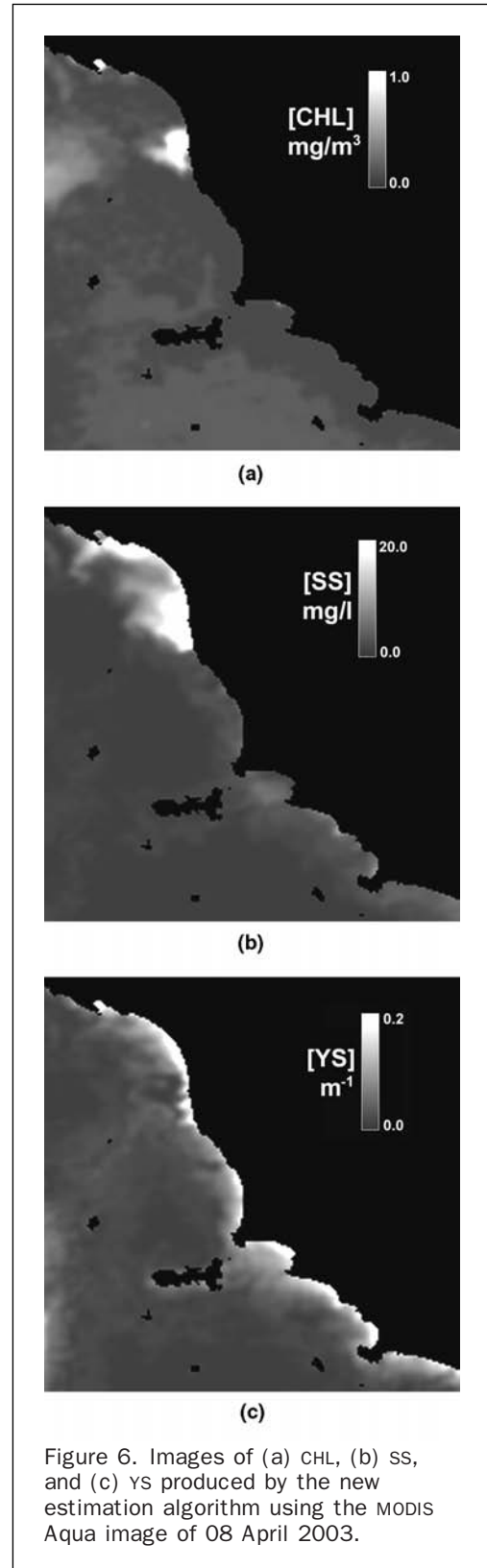
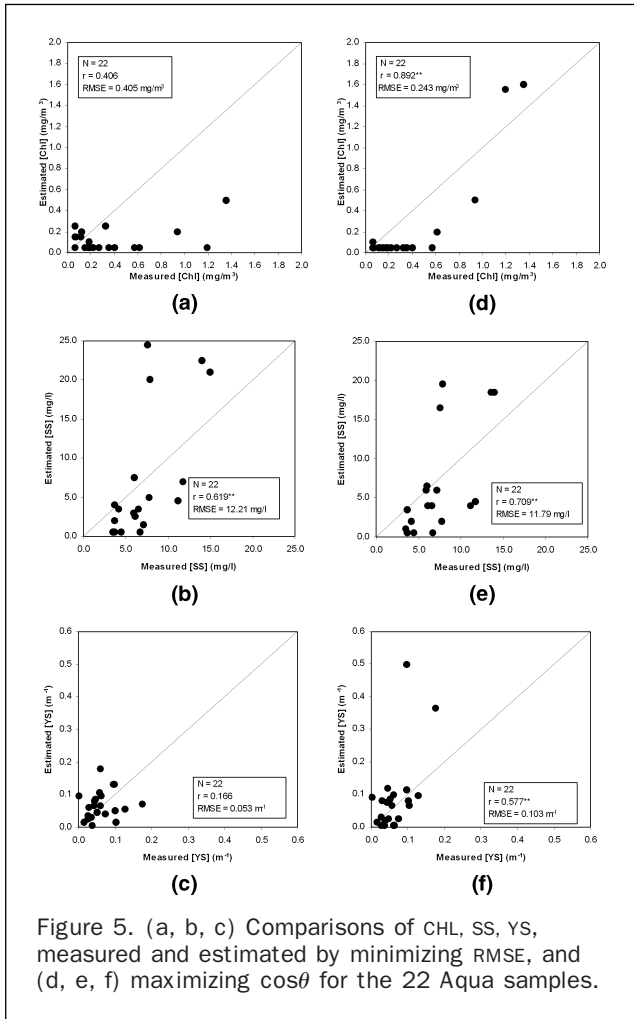
concentrations of all three main optically active seawater constituents, which is instead possible by classical inversion methods (Maritorea *et al.*, 2002).

A modification of classical inversion algorithms was therefore proposed, based on the computation of a new index of similarity between measured and simulated reflectance spectra. This index, the cosine of the spectral angle, is intrinsically insensitive to reflectance amplitude variations and is instead dependent on shape spectral variations.

From a theoretical viewpoint, the use of such an index in place of the classical $RMSE_{M,S}$ presents possible advantages and drawbacks. The exclusive sensitivity to varia-

tions in spectral shape can in fact reduce the influence of the mentioned problems, but at the expense of a loss of the information related to important amplitude variations. The final effect of the proposed modification will therefore depend on the balance between these two factors, which will in turn be related to the proportional information content brought by amplitude and shape variations on the concentrations of the various seawater constituents.

The proposed modification will therefore produce significant improvements over the classical approach only in cases where amplitude spectral variations of the observed signal mainly contain noise and are poorly informative on



constituent concentrations. This situation may be common in Case 2 waters, where the effects of the complex interactions among the main optically active constituents are usually summed to the consequences of inaccurate atmospheric corrections (Darecky and Stramsky, 2004).

The effectiveness of the proposed modification was subjected to experimental verification using *in situ* and MODIS data taken in optically complex coastal waters. The information brought by the new error index on the concentrations of optically active seawater constituents was first evaluated with respect to that of a conventional index using sea and satellite data taken in the Tuscany Sea during 2003. The accuracy of inversion algorithms based on the two indices was then assessed to estimate the same concentrations. The tests performed indicated the superiority of the new method, particularly for the estimation of CHL. This implies that, in the specific case study, the above mentioned conditions for the proficient application of the new error index are mostly met.

The same experimental results showed some weaknesses of the new method. A slight underestimation persisted for CHL, while SS and YS were variably estimated. Also these findings may be explained by the previous considerations on the information brought by amplitude and shape spectral reflectance variations. In fact, the reflectance amplitude variations found in the examined seawater samples are partly determined by varying concentrations of SS and YS. Consequently, disregarding such

variations inevitably leads to losing partially useful information on these concentrations. This is less the case for CHL, which has only a minor impact on seawater reflectance amplitude variability but significantly determines reflectance shape variations.

A major limit of the current experiment was due to the small number of samples used for the data analysis. This limit mainly came from the nature of the sea data collection, which was not specifically planned for the current research. Due to the limited number of samples, the results obtained can not be considered statistically conclusive. Moreover, they might be representative only for particular environmental conditions, and their extendibility to other cases should be tested by further experiments. Since the potential of the new algorithm critically depends on the correct definition of spectral shapes, its application is expected to benefit from the increased information which should be contained in higher-dimensional hyperspectral data. This expectation too should be substantiated by appropriate experimental activities, which should use specifically collected ground and satellite data.

Acknowledgments

The authors thank two anonymous PE&RS referees for their comments which significantly improved the quality of the original manuscript.

References

- Ahn, Y.H., J.E. Moon, and S. Gallegos, 2001. Development of suspended particulate matter algorithms for ocean color remote sensing, *Korean Journal of Remote Sensing*, 17(4):285–295.
- Babin, M., D. Stramski, G.M. Ferrari, H. Claustre, A. Bricaud, G. Obolensky, and N. Hoepffener, 2003a. Variation in the light absorption coefficients of phytoplankton, non algal particles, and dissolved organic matter in coastal waters around Europe, *Journal of Geophysical Research*, 108:3211–3231.
- Babin, M., A. Morel, V. Fournier-Sicre, F. Fell and D. Stramski, 2003b. Light scattering properties of marine particles in coastal and open ocean waters as related to particle mass concentration, *Limnology and Oceanography*, 48(2):843–859.
- Bailey, S.W., and P.J. Werdell, 2006. A multi-sensor approach for the on-orbit validation of ocean color satellite data products, *Remote Sensing of Environment*, 102:12–23.
- Bricaud, A., A. Morel, and L. Prieur, 1981. Absorption by dissolved organic matter of the sea (yellow substance) in the UV and visible domains, *Limnology and Oceanography*, 26(1):43–53.
- Bricaud, A., and D. Stramski, 1990. Spectral absorption coefficients of living phytoplankton and nonalgal biogenous matter: A comparison between Peru upwelling area and the Sargasso Sea, *Limnology and Oceanography*, 35(3):562–582.
- Carder, K.L., F.R. Chen, Z. Lee, S.K. Hawes, and J.P. Cannizzaro, 2003. *Case 2 Chlorophyll_a, Algorithm and Case 2 Absorption Coefficient Algorithm, ATBD (MOD 19)*, Version 7, College of Marine Science, University of South Florida, St. Petersburg, Florida.
- Carder, K.L., F.R. Chen, J.P. Cannizzaro, J.W. Campbell, and B.G. Mitchell, 2004. Performance of the MODIS semi-analytical ocean color algorithm for chlorophyll-a, *Advances in Space Research*, 33:1152–1159.
- Chang, G.C., T.D. Dickey, S. Jiang, D.V. Manov, and F.W. Spada, 2003. Optical methods for interdisciplinary research in the coastal ocean, *Recent Research Developments in Optics* (M. Kawasaki, N. Ashgriz, and R. Anthony, editors), Research Signpost, India, 3, pp. 249–270.
- Chang, G.C., A.H. Barnard, S. McLean, P.J. Egli, C. Moore, J.R.V. Zaneveld, T.D. Dickey, and A. Hanson, 2006. *In situ* optical variability and relationships in the Santa Barbara Channel: implications for remote sensing, *Applied Optics*, 45(15):3593–3604.
- Darecki, M., and D. Stramski, 2004. An evaluation of MODIS and SeaWiFS bio-optical algorithms in the Baltic Sea, *Remote Sensing of Environment*, 89:326–350.
- Davies-Colley, R.J., and W.N. Vant, 1987. Absorption of light by yellow substance in freshwater lakes, *Limnology and Oceanography*, 32:416–425.
- Gordon, H.R., O.B. Brown, and M.M. Jacobs, 1975. Computed relationships between the inherent and apparent optical properties of a flat homogeneous ocean, *Applied Optics*, 14:417–427.
- Holm-Hansen, O., C.J. Lorenzen, R.W. Holmes, and J.D.H. Strickland, 1965. Fluorometric determination of chlorophyll, *Journal du Conseil*, 30(1):3–15.
- Innamorati, M., C. Nuccio, L. Lazzara, G. Mori, L. Massi, and M. De Pol, 1993. Condizioni trofiche, biomassa e popolamenti fitoplanctonici dell'Alto Tirreno, *Progetto Mare, Ricerca sullo stato Biologico, Chimico e Fisico dell'Alto Tirreno Toscano*, Regione Toscana, Università di Firenze, C. Nuccio, Dipartimento di Biologia Vegetale, University Firenze, pp. 103–156.
- Innamorati, M., G. Mori, C. Nuccio, L. Massi, C. Melillo, M. Mannucci, B. Terreri, A. De Pasquale, and F. Polonelli, 2003. Indagine sulle mucillaggini nel Mar Tirreno, Progetto di studio coordinato dall'ICRAM, *Processi di Formazione delle Mucillaggini nell'Adriatico e nel Tirreno - MAT*, rapporto finale ICRAM.
- IOCCG, 2000. Remote sensing of ocean colour in coastal, and other optically-complex, waters (S. Sathyendranath, editor), *Reports of the International Ocean-Colour Coordinating Group, 3*, IOCCG, Dartmouth, Canada.
- IOCCG, 2006. Remote sensing of inherent optical properties: Fundamentals, tests of Algorithms, and Applications (Z.P. Lee, editor), *Reports of the International Ocean-Colour Coordinating Group, 5*, IOCCG, Dartmouth, Canada.
- IPCC, 2001. Climate change 2001. *IPCC Third Assessment Report*, URL: http://www.grida.no/climate/ipcc_tar/, (last date accessed: 03 February 2009).
- Kirk, J.T.O., 1989. Upwelling light stream in natural waters, *Limnology and Oceanography*, 34(8): 1410–1425.
- Kirk, J.T.O., 1994. *Light and Photosynthesis in Aquatic Ecosystems*, Second edition, Cambridge University Press.
- Kishino, M., N. Okami, M. Takahashi, and S. Ichimura, 1985. Light utilization efficiency and quantum yield of phytoplankton in a thermally stratified sea, *Limnology and Oceanography*, 31:557–566.
- Lee, Z., and K.L. Carder, 2002. Effect of spectral band numbers on the retrieval of water column and bottom properties from ocean color data, *Applied Optics*, 41(12):2191–2201.
- Loisel, H., and D. Stramski, 2000. Estimation of the inherent optical properties of natural waters from the irradiance attenuation coefficient and reflectance in the presence of Raman scattering, *Applied Optics*, 39(18):3001–3011.
- Maritorena, S., D.A. Siegel, and A.R. Peterson, 2002. Optimization of a semianalytical ocean color model for global-scale applications, *Applied Optics*, 41(15):2002.
- Maselli, F., L. Massi, C. Melillo, and M. Innamorati, 2005. Unsupervised spectral characterization of shallow lagoon waters by the use of Landsat TM and ETM+ data, *Photogrammetric Engineering & Remote Sensing*, 71(11):1265–1274.
- Mobley, C.D., 1994. *Light and Water - Radiative Transfer in Natural Waters*, Academic Press, San Diego, USA, 592 p.
- Morel, A., and L. Prieur, 1977. Analysis of variations in ocean color, *Limnology and Oceanography*, 22:709–722.
- Morel, A., and B. Gentili, 1996. Diffuse reflectance of oceanic waters - III, Implication of bidirectionality for the remote-sensing problem, *Applied Optics*, 35(24):4850–4862.
- Morel, A., and S. Bélanger, 2006. Improved detection of turbid waters from ocean color sensors information, *Remote Sensing of Environment*, 102:237–249.
- Mueller, J.L., and R.W. Austin, 1995. *Ocean Optics Protocols for SeaWiFS: Validation, Revision 1*, SeaWiFS Technical Report Series 25 (S.B. Hooker, E.R. Firestone and J.G. Acker, editors), NASA Technical Memorandum 104566, Greenbelt, Maryland.
- O'Reilly, J.E., S. Maritorena, B.G. Mitchell, D.A. Siegel, K.L. Carder, S.A. Garver, M. Kahru, and C. McClain, 1998. Ocean color chlorophyll algorithms for SeaWiFS, *Journal of Geophysical Research*, 103(C11):24937–24953.
- O'Reilly, J.E., S. Maritorena, D. Siegel, M.C. O'Brien, D. Toole, B.G. Mitchell, M. Kahru, F.P. Chavez, P. Strutton, G. Cota,

- S.B. Hooker, C.R. McClain, K.L. Carder, F. Muller-Karger, L. Harding, A. Magnuson, D. Phinney, G.F. Moore, J. Aiken, K.R. Arrigo, R. Letelier, and M. Culver, 2000. Ocean color chlorophyll a algorithms for SeaWiFS, OC2, and OC4: Version 4, *SeaWiFS Postlaunch Calibration and Validation Analyses, Part 3* (S.B. Hooker and E.R. Firestone, editors), NASA Technical Memorandum 2000-206892, Vol. 11, NASA Goddard Space Flight Center, Greenbelt, Maryland, pp. 9–23.
- Ouillon, S., and A.A. Petrenko, 2005. Above-water measurements of reflectance and chlorophyll-a algorithms in the Gulf of Lions, NW Mediterranean Sea, *Optics Express*, 13(7):2531–2548.
- Pope, R.M., and E.S. Fry, 1997. Absorption spectrum (380–700) of pure water - II: Integrating cavity measurements, *Applied Optics*, 36(33):8710–8723.
- Ruddick, K.G., V. De Cauwer, Y.J. Park, and G. Moore, 2006. Seaborne measurements of near infrared water-leaving reflectance: The similarity spectrum for turbid waters, *Limnology and Oceanography*, 51(2):1167–1179.
- Santini, C., M. Pieri, E. Santoro, L. Massi, and F. Maselli, 2004. Analisi di dati MERIS e MODIS nello studio delle acque marino costiere della Regione Toscana, *Atti della 8a Conferenza Nazionale ASITA, GEOMATICA Standardizzazione, Interoperabilità e Nuove tecnologie*, 14–17 Dicembre, Roma.
- Siegel, D.A., M. Wang, S. Maritorena, and W. Robinson, 2000. Atmospheric correction of satellite ocean color imagery: The black pixel assumption, *Applied Optics*, 39:3582–3591.
- Shanmugan, P., and Y.H. Ahn, 2007. New atmospheric correction technique to retrieve the ocean colour from SeaWiFS imagery in complex coastal waters, *Journal of Optics A: Pure and Applied Optics*, 9:511–530.
- Smith, R.C., and K.S. Baker, 1981. Optical properties of the clearest natural waters, *Applied Optics*, 20:177–184.
- Sohn, Y., and N.S. Rebello, 2002. Supervised and unsupervised spectral angle classifiers, *Photogrammetric Engineering & Remote Sensing*, 68(12):1271–1280.
- Strickland, J.D.H., and T.R. Parson, 1972. A practical handbook of sea-water analysis, *Journal of the Fisheries Research Board of Canada*, 177–179.
- Tassan, S., and G.M. Ferrari, 1995. An alternative approach to absorption measurement of aquatic particles retained on filters, *Limnology and Oceanography*, 40(8):1358–1368.
- Vaillancourt, R.D., C.W. Brown, R.R.L. Guillard, and W.M. Balch, 2004. Light backscattering properties of marine phytoplankton: Relationships to cell size, chemical composition and taxonomy, *Journal of Plankton Research*, 26(2):191–212.
- Van der Linde, D.W., 1998. *Protocol for Determination of Total Suspended Matter in Oceans and Coastal Zones*, CEC-JRC-Ispra, Technical note I., 98, 182 p.
- Volpe, G., R. Santoleri, V. Vellucci, M. Ribera d'Alcalà, S. Marullo, and F. D'Ortenzio, 2007. The colour of the Mediterranean Sea: Global versus regional bio-optical algorithms evaluation and implication for satellite chlorophyll estimates, *Remote Sensing of Environment*, 107(4):625–638.
- Zawada, D.G., C. Hu, T. Clayton, Z. Chen, J.C. Brock, and F. Muller-Karger, 2007. Remote sensing of particle back-scattering in Chesapeake Bay: A 6-year SeaWiFS retrospective view, *Estuarine Coastal and Shelf Science*, 73:792–806.
- Zibordi, G., F. Mélin, and J.-F. Berthon, 2006. Comparison of SeaWiFS, MODIS and MERIS radiometric products at a coastal site, *Geophysical Research Letters*, 33(L06617):1–4.